Hindawi
International Journal of Mathematics and Mathematical Sciences
Volume 2018, Article ID 7019868, 18 pages
https://doi.org/10.1155/2018/7019868

Research Article

Mathematical Model for Hepatocytic-Erythrocytic Dynamics of Malaria

Titus Okello Orwa, Rachel Waema Mbogo, and Livingstone Serwadda Luboobi

Institute of Mathematical Sciences, Strathmore University, P.O. Box 59857-00200, Nairobi, Kenya

Correspondence should be addressed to Titus Okello Orwa; torwa@strathmore.edu

Received 23 October 2017; Accepted 20 May 2018; Published 2 July 2018

Academic Editor: Niansheng Tang

Human malaria remains a major killer disease worldwide, with nearly half (3.2 billion) of the world's population at risk of malaria infection. The infectious protozoan disease is endemic in tropical and subtropical regions, with an estimated 212 million new cases and 429,000 malaria-related deaths in 2015. An in-host mathematical model of *Plasmodium falciparum* malaria that describes the dynamics and interactions of malaria parasites with the host's liver cells (hepatocytic stage), the red blood cells (erythrocytic stage), and macrophages is reformulated. By a theoretical analysis, an in-host basic reproduction number R_0 is derived. The disease-free equilibrium is shown to be locally and globally asymptotically stable. Sensitivity analysis reveals that the erythrocyte invasion rate β_r, the average number of merozoites released per bursting infected erythrocyte K, and the proportion of merozoites that cause secondary invasions at the blood phase ζ are the most influential parameters in determining the malaria infection outcomes. Numerical results show that macrophages have a considerable impact in clearing infected red blood cells through phagocytosis. Moreover, the density of infected erythrocytes and hence the severity of malaria are shown to increase with increasing density of merozoites in the blood. Concurrent use of antimalarial drugs and a potential erythrocyte invasion-avoidance vaccine would minimize the density of infected erythrocytes and hence malaria disease severity.

1. Introduction

Human malaria remains a major killer disease worldwide, with nearly half (3.2 billion) of the world's population at risk of malaria infection [1]. The infectious disease is endemic in tropical and subtropical regions, with an estimated 212 million new cases (uncertainty range: 148–304 million) and 429,000 malaria-related deaths (range: 235,000–639,000) in 2015 [2]. 92% of the deaths and 90% of the cases occurred in sub-Saharan Africa. 70% of the reported deaths occurred among children below the age of five. Despite existing vector control measures and tremendous progress in the development of antimalarial therapy accompanied with worldwide decline in incidence rate (fell by 21% in 2015) and mortality rate (fell by 29% in 2015), malaria remains one of the greatest global health challenges to date [2].

The protozoan disease is caused by parasites of the genus *Plasmodium* which are transmitted to humans by the bite of female *Anopheles* mosquito. *Plasmodium falciparum*, which is predominant in sub-Saharan Africa, New Guinea, and Haiti [3], is the major cause of malaria infections. The other *Plasmodium* species that cause malaria are *P. vivax*, *P. ovale*, *P. malariae*, and *P. knowlesi* [4]. *P. vivax* and *P. ovale* can hide in the liver for prolonged periods as hypnozoites, causing relapsing malaria months or even years after the initial infection [5]. *P. vivax* has the greatest geographical range of the disease and hence is the main contributor to worldwide malaria morbidity [3]. Our study focuses on the dynamics of *Plasmodium falciparum* in the human host.

During their obligatory blood meals, infected female *Anopheles* mosquitoes inject sporozoites belonging to *Plasmodium falciparum* species into the human dermis [6]. The motile sporozoites travel through the blood vessels and enter the host's liver. Hepatocyte invasion is accompanied by the formation of parasitophorous vacuole (PV) around the sporozoite [7]. They form preerythrocytic schizonts and multiply by schizogony, culminating in the production of 8–24 first generation merozoites that are released into the

blood when the liver schizonts burst open [8]. The released merozoites invade susceptible erythrocytes and undergo another phase of schizogony, which is relatively faster compared to that at the exoerythrocytic stage [9].

Within a period of two days, the infected red blood cells rupture to release about 16 daughter merozoites [10]. Most of the released merozoites quickly invade susceptible erythrocytes, leading to another cycle of infections. The waves of bursting erythrocytes and the invasion of fresh erythrocytes by the newly released merozoites increase parasitemia and produce malaria's characteristic symptoms [11]. In the absence of adequate protective immune response or antimalarial therapy, the host is likely to suffer severe anaemia or even die [12]. The rest of the daughter merozoites develop into sexual forms called gametocytes [10]. These gametocytes are later taken up by other female *Anopheles* mosquitoes during feeding [13]. This marks the beginning of the sporogenic cycle that occurs within the mosquito vector.

The presence of the malaria parasites in the human body elicits response from numerous immune cells. The innate immune system and the adaptive immune system form the first and the second lines of defence, respectively [14]. Adaptive immune system further provides protection against future exposures to malaria pathogens. Innate immune cells such as the *Plasmodium falciparum* DNA, natural killer cells (NK cells), dendritic cells (DCs), macrophages, natural killer T (NKT) cells, and T cells are involved in the clearance of circulating parasites, infected erythrocytes, and infected hepatocytes [14]. Subject to parasite strain, the DCs and NK cells may prompt or restrain inflammatory responses [15]. The NKT cells also help regulate DCs and T cell responses to *Plasmodium* [14]. Moreover, studies in [16] have demonstrated that malaria infection induces activation of Toll-like receptors (TLRs): TLR1, TLR2, TLR4 (which are located on the cell surface), and TLR9 which is not expressed on the cell surface. TLR2 and TLR9 are also activated by malarial glycosylphosphatidylinositol (GPI) anchors and parasite-derived DNA bound to hemozoin [16].

Unlike the NK cells, the macrophages have been shown to effectively phagocytose malaria-infected red blood cells during the erythrocytic phase [17]. A part from its ability to wholly ingest infected red blood cells, the macrophages can also selectively extract malaria parasites from recently infected erythrocytes [18]. The parasite-extraction capability of macrophage therefore leaves the surviving erythrocytes to continue circulating like the other healthy red blood cells.

The rest of the paper is organized as follows: in Section 2, we formulate the in-host malaria model and state the invariant region in which the model is defined. In Section 3, we compute and describe the model in-host reproduction number. The results on model equilibrium points (disease-free equilibrium and endemic equilibrium points) and the stability of the disease-free equilibrium point are also considered in Section 3. Section 4 is devoted to numerical solution of the in-host model under different conditions of the threshold parameter (in-host reproduction number). Parameter sensitivity analysis and the effects of parameter variation on different populations are investigated in Section 4. A conclusion and discussion complete the paper in Section 5.

2. In-Host Malaria Model

Several studies on mathematical modelling of in-host malaria and its dynamics within the human host have been done. Nearly all the earlier mathematical models (see, e.g., [25–27]) focused on improving *Plasmodium falciparum* control while focusing on the blood stage of parasite development. These models have been found to be useful in explaining in-host observations by means of biologically plausible assumptions such as parasite diversity, predicting the impact of interventions or the use of antimalarials [28], and estimating hidden parameter values [29]. Although the models in [19, 21, 23, 30] have considered the impact of immune response and treatment, the modelling is only limited to the blood stage of *Plasmodium falciparum* development. In [20, 22, 31], the liver stage is incorporated in the malaria model. However, the contribution of immune system is ignored in [20, 31]. Moreover, all the immune cells are assumed to play an active role during malaria infection in [22]. This may not be entirely true. The specific impacts of immune responses to malaria infection are well discussed in [32–36].

In the following sections, we extended the model in [21] by incorporating the liver stage of parasite development. The reformulated in-host malaria model focuses on the erythrocytic and hepatocytic stages and describes the dynamics of interactions between the malaria parasites, the liver hepatocytes, the red blood cells, and the macrophages (immune system cells). Unlike the work in [20, 22], we ignored the vector stage of parasite development and assumed a twofold process in the generation of hepatocytes: from the bone marrow and from self-replication of the existing hepatocytes. Again, we have assumed that the generation of macrophages and the susceptible red blood cells from the bone marrow increase with increasing density of the infected erythrocytes. However, whatever density of the infected erythrocytes, there is a limit on the rate at which cells can be released from the bone marrow.

2.1. Model Formulation. The hepatocytic-erythrocytic malaria model describes the dynamics of *Plasmodium falciparum* parasite during the hepatocytic and erythrocytic stages and their interactions with the host's red blood cells, liver hepatocytes, and the macrophages. The compartmental model assumes seven interacting populations of sporozoites $S(t)$, susceptible hepatocytes $H(t)$, infected hepatocytes $H_X(t)$, susceptible red blood cells (RBCs) $R(t)$, infected red blood cells (IRBCs) $R_X(t)$, merozoites $M(t)$, and macrophages $Z(t)$ at any time t. The dynamics of malaria parasites and host-cell populations in each compartment are described as follows.

Sporozoites (S). The female *Anopheles* mosquito is assumed to inject sporozoites into the human system during blood meal at a constant rate Λ. The sporozoites molt through the blood stream and reach the liver in about 2 hours, where they invade the hepatocytes at the rate β_s. We assume that the sporozoites can die naturally at a rate δ_s.

Susceptible Hepatocytes (H). We consider the bone marrow and self-replication as the main sources of the liver hepatocytes. The recruitment of hepatocytes from the bone marrow is assumed to occur at a constant rate λ_h. Just like during liver transplant [37], we argue that, during severe malaria infections, the rate of generation of healthy hepatocytes is likely to increase tremendously and in proportion to the concentrations of the infected liver cells [38]. This additional increase is represented by the term $\rho_1 H_X/(\kappa_1 + H_X) = \psi_1(H_X)$, where H_X and ρ_1, respectively, represent the concentration of infected hepatocytes and their rates of generation. The parameter κ_1 represents the number/concentration of the infected hepatocytes at which the recruitment of the healthy hepatocytes is a half of the maximum rate. Owing to invasion by sporozoites at the rate β_s, susceptible hepatocytes get infected and progress to subpopulation H_X. In addition, hepatocytes in compartment H are assumed to have a natural life expectancy and may hence die naturally at the rate μ_1.

Infected Hepatocytes (H_X). Infected hepatocytes mature into liver-stage schizonts. These schizonts burst open releasing 2000–40000 uninucleate merozoites into the blood stream [39]. The term $N\mu_2 H_X$ represents the total population of merozoites released upon bursting of infected hepatocytes. The parameter μ_2 represents the death rate of the infected hepatocytes.

Susceptible Red Blood Cells (R). Similar to malaria models in [21, 23, 30], we have assumed that the susceptible RBCs get recruited at a constant rate λ_r from the bone marrow. We further assume that, during infection, the erythrocyte production is accelerated owing to the presence of IRBCs at the rate ρ_2. This increase is denoted by the term $\rho_2 R_X/(\kappa_2 + R_X) = \psi_2(R_X)$, where κ_2 represents number/concentration of the infected red blood cells at which the recruitment of susceptible red blood cells is a half of the maximum rate. The particular mechanisms involved in this accelerated process are, however, still poorly understood [40]. The susceptible RBCs get infected by merozoites at a rate proportional to the contact rate of their density, $\beta_r MR$. The positive constant β_r describes the rate of successful invasion by a malaria merozoite. The susceptible RBCs die naturally at a rate μ_3.

Infected Red Blood Cells (R_X). Upon invasion by merozoites, the healthy RBCs get infected, leading to the formation of infected red blood cells R_X. Although the RBCs die at a constant rate μ_4, they can similarly be killed through phagocytosis by the macrophages at the rate η. At maturity, the IRBCs burst open, releasing free merozoites into the blood system, causing secondary invasion and disease progression.

Merozoites (M). After 2–15 days, the infected hepatocytes burst open and release merozoites into the blood system. This is represented by the term $N\mu_2 H_X$, where N is the average number of merozoites released per bursting infected hepatocytes. An average of K merozoites is released per each bursting IRBC. These free parasites suffer a natural death at a rate δ_m and invade susceptible RBCs at a rate β_r. Within the red blood cells, the merozoites mature either into uninucleate

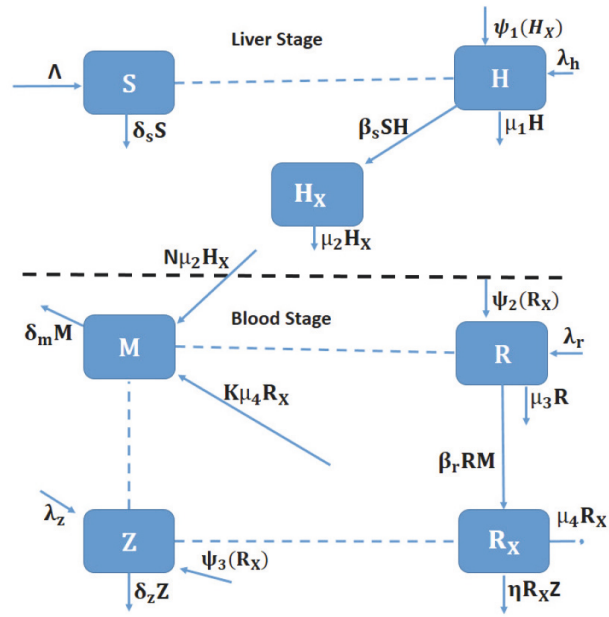

Figure 1: Schematic diagram for hepatocytic-erythrocytic and malaria parasite dynamics. The dotted lines without arrows indicate cell-parasite interaction and the solid lines show progression from one compartment to another.

gametocyte or into erythrocytic stage schizont containing 10–36 merozoites [39]. After about 48–72 hours, the erythrocytic stage schizont ruptures, releasing more merozoites into blood stream to cause further invasion of healthy RBCs. We assume that a proportion ζ of the merozoites contribute to secondary invasion of the susceptible RBCs. The rest of the merozoites $(1 - \zeta)$ transform into gametocytes that are later picked up by female *Anopheles* mosquitoes during feeding.

Macrophages (Z). Owing to their effectiveness in elimination of infected erythrocytes and infective malaria parasites, we have considered the innate macrophage cells as the main part of the immune response in malaria infection. Consequently, we have assumed that the macrophage cells are recruited at a constant rate λ_z from the bone marrow. Moreover, they proliferate at a rate ρ_3 in the sites of infection in proportion to the density of IRBCs. This is represented by the term $\rho_3 R_X/(\kappa_3 + R_X) = \psi_3(R_X)$, where κ_3 denotes the number/concentration of the infected red blood cells at which the recruitment of the macrophages is a half of the maximum rate. We further assume that they can die naturally at a constant rate δ_z.

The variables and parameters that describe in-host malaria dynamics are as in Tables 1 and 2, respectively.

The above transmission dynamics of malaria are summarised in the compartmental diagram in Figure 1.

From the above description of the in-host dynamics of malaria and the representation in Figure 1, we derive the following system of ordinary differential equations:

$$\frac{dH}{dt} = \lambda_h + \frac{\rho_1 H_X}{\kappa_1 + H_X} - \mu_1 H - \beta_s SH,$$

Table 1: Symbols and definition of state variables considered in the model.

Variable	Description
$H(t)$	The population of susceptible hepatocytes at time t
$H_X(t)$	The population of infected hepatocytes at time t
$R(t)$	The population of susceptible red blood cells (erythrocytes) at time t
$R_X(t)$	The population of infected red blood cells at time t
$Z(t)$	The density of macrophages in the human body at time t
$S(t)$	The population of sporozoites at time t
$M(t)$	The population of merozoites at time t

Table 2: Symbols and description of parameters used in the model.

Parameter	Description
Λ	The total rate of injection of sporozoites into liver due to mosquito bites
δ_s	The death rate of sporozoites
λ_h	Recruitment rate of susceptible hepatocytes from the bone marrow
μ_1	Natural death rate of susceptible hepatocytes
β_s	The invasion rate of hepatocytes by sporozoites
μ_2	Death rate of infected hepatocytes
λ_r	Recruitment rate of susceptible RBCs by the bone marrow
μ_3	The natural death rate of RBCs
β_r	The invasion rate of RBCs by merozoites
μ_4	Death rates of IRBCs
δ_m	The death rate of merozoites
λ_z	Recruitment rate of macrophages from the bone marrow
δ_z	The death rate of a macrophage
η	Elimination rate of IRBCs by macrophages
ρ_1	Production rate of hepatocytes due to presence of infected hepatocytes
ρ_2	Production rate of RBCs due to presence of IRBCs
ρ_3	Immunogenicity of IRBCs
κ_1	Number of H_X at which the recruitment of H is a half of the maximum rate
κ_2	Number of R_X at which the recruitment of R is a half of the maximum rate
κ_3	Number of R_X at which the recruitment of Z is a half of the maximum rate
ζ	The proportion of the merozoites that cause secondary infections
K	The average number of merozoites released per bursting IRBCs
N	The average number of merozoites released per bursting infected hepatocytes

$$\begin{aligned}
\frac{dH_X}{dt} &= \beta_s SH - \mu_2 H_X,\\
\frac{dR}{dt} &= \lambda_r + \frac{\rho_2 R_X}{\kappa_2 + R_X} - \mu_3 R - \beta_r RM,\\
\frac{dR_X}{dt} &= \beta_r RM - \mu_4 R_X - \eta R_X Z,\\
\frac{dZ}{dt} &= \lambda_z + \frac{\rho_3 R_X}{\kappa_3 + R_X} - \delta_z Z,\\
\frac{dS}{dt} &= \Lambda - \delta_s S - \beta_s SH,\\
\frac{dM}{dt} &= N\mu_2 H_X + K\zeta\mu_4 R_X - \delta_m M - \beta_r RM,
\end{aligned} \tag{1}$$

where $H(0) \geq 0$, $H_X(0) \geq 0$, $R(0) \geq 0$, $R_X(0) \geq 0$, $Z(0) \geq 0$, $S(0) \geq 0$, and $M(0) \geq 0$.

3. Model Analysis

3.1. Basic Properties. In this section, we study whether the formulated model (1) is biologically and mathematically meaningful. We establish model equilibrium points and investigate their stability properties.

3.1.1. Well-Posedness of the Model. For the in-host malaria model (1) to be mathematically and biologically meaningful, we need to prove that all the solutions of model system (1) with nonnegative initial conditions would remain nonnegative for all time $t \geq 0$. Positivity in the model is shown by proving the following theorem.

Theorem 1. *Let the parameters in model (1) be positive constants. A nonnegative solution* $(H(t), H_X(t), R(t), R_X(t), Z(t), S(t), M(t))$ *exists for all the state variables with nonnegative initial conditions* $\{H(0) = H_0 \geq 0,\ H_X(0) = H_{X0} \geq 0,\ R(0) = R_0 \geq 0,\ R_X(0) = R_{X0} \geq 0,\ Z(0) = Z_0 \geq 0,\ S(0) = S_0 \geq 0,\ M(0) = M_0 \geq 0\} \forall t \geq 0$.

Proof. Considering the first equation in system (1), let $\psi_1(t) = \rho_1 H_X/(\kappa_1 + H_X)$, so that

$$\begin{aligned} \frac{\mathrm{d}H}{\mathrm{d}t} &= \lambda_h + \varphi(t) - \mu_1 H - \beta_s S H, \\ \frac{\mathrm{d}H}{\mathrm{d}t} &\geq -(\mu_1 + \beta_s S) H, \end{aligned} \tag{2}$$

which yields

$$H(t) \geq H(0) \exp\left\{-\left(\int_0^t \beta_s S(s)\, ds + \mu_1 t\right)\right\} > 0. \tag{3}$$

In a similar fashion, this procedure can be applied to all the remaining six equations in model system (1), so that we have the following solutions:

$$\begin{aligned} H_X(t) &\geq H_X(0) \exp\{-\mu_2 t\} > 0, \\ R(t) &\geq R(0) \exp\left\{-\left(\int_0^t \beta_r M(s)\, ds + \mu_3 t\right)\right\} > 0, \\ R_X(t) &\geq R_X(0) \exp\left\{-\left(\int_0^t \eta Z(s)\, ds + \mu_4 t\right)\right\} > 0, \\ Z(t) &\geq Z(0) \exp\{-\delta_z t\} > 0, \\ S(t) &\geq S(0) \exp\left\{-\left(\int_0^t \beta_s H(s)\, ds + \delta_s t\right)\right\} > 0, \\ M(t) &\geq M(0) \exp\left\{-\left(\int_0^t \beta_r R(s)\, ds + \delta_m t\right)\right\} > 0. \end{aligned} \tag{4}$$

Therefore, state variables $(H, H_X, R, R_X, Z, S, M)$ of model system (1) are nonnegative for all time $t > 0$. □

3.1.2. Invariant Region. Let $N_H(t)$ represent the total hepatocyte population, so that $N_H(t) = H(t) + H_X(t)$.

On substituting the derivatives in system (1) and simplifying, we have

$$\frac{dN_H}{dt} \leq \lambda_h + \psi_1(t) - \mu_h N_H, \tag{5}$$

where $\psi_1(t) = \rho_1 H_X/(\kappa_1 + H_X)$ and $\mu_h = \min\{\mu_1, \mu_2\}$.

Using integrating factor $e^{\mu_h t}$,

$$N_H(t) \leq \frac{\lambda_h}{\mu_h} + e^{-\mu_h t} \int_0^t \psi_1(\tau)\, e^{\mu_h \tau} d\tau + c_1 e^{-\mu_h t}, \tag{6}$$

where c_1 is a constant of integration. By applying the initial condition $N_H(0) = N_{H0} > 0$ in (6), we obtain

$$c_1 = \left(N_H(0) - \frac{\lambda_h}{\mu_h}\right) - \int_0^t \psi_1(\tau)\, e^{-\mu_h \tau} d\tau. \tag{7}$$

Substituting the value of c_1 into $N_H(t)$ in (6) and simplifying, we get

$$N_H(t) \leq \frac{\lambda_h}{\mu_h} + e^{-\mu_h t}\left(N_H(0) - \frac{\lambda_h}{\mu_h}\right). \tag{8}$$

There are two possible cases in analyzing the behaviour of $N_H(t)$ in (8). In the first case, we consider $N_H(0) > \lambda_h/\mu_h$ so that, at time $t = 0$, the right-hand side (RHS) of (8) experiences the largest possible value of $N_H(0)$. That is, $N_H(t) \leq N_H(0)$ for all time $t > 0$.

In the second case, we consider $N_H(0) < \lambda_h/\mu_h$, so that the largest possible value of the RHS of (8) approaches λ_h/μ_h as time t goes to infinity. Thus, $N_H(t) \leq \lambda_h/\mu_h$, $\forall t > 0$. From these two cases, we conclude that $N_H(t) \leq \max\{N_H(0), \lambda_h/\mu_h\}$ for all time $t > 0$.

Using the above approach, let the total red blood cells population be $N_R(t)$, so that $N_R(t) = R(t) + R_X(t)$. From the model equations in system (1), we have

$$\frac{dN_R}{dt} \leq \lambda_r + \psi_2(t) - \mu_r N_R(t), \tag{9}$$

where $\psi_2(t) = \rho_2 R_X/(\kappa_2 + R_X)$ and $\mu_r = \min\{\mu_3, \mu_4\}$. Upon solving for N_R in (9), we have $N_R(t) \leq \max\{N_R(0), \lambda_r/\mu_r\}$, $\forall t > 0$.

For the macrophage compartment $Z(t)$, we have

$$\frac{\mathrm{d}Z}{\mathrm{d}t} = \lambda_z + \psi_3(t) - \delta_z Z, \quad \text{for } \psi_3(t) = \frac{\rho_3 R_X}{\kappa_3 + R_X}. \tag{10}$$

By integration, the solution of (10) is presented as

$$Z(t) \leq \frac{\lambda_z}{\delta_z} + e^{-\delta_z t}\left(Z(0) - \frac{\lambda_z}{\delta_z}\right). \tag{11}$$

By inspection, $Z(t) \leq \max\{Z(0), \lambda_z/\delta_z\}$ for all time $t > 0$.

Finally, let $N_P(t)$ represent the total population of malaria parasites at any time t. That is, $N_P(t) = S(t) + M(t)$ and, from system (1),

$$\begin{aligned} \frac{\mathrm{d}N_P}{\mathrm{d}t} &= \Lambda - \delta_s S - \beta_s S H + N\mu_2 H_X + K\zeta\mu_4 R_X \\ &\quad - \delta_m M, \leq \Lambda + (K\zeta\mu_4 R_X + N\mu_2 H_X) - \delta_p N_p, \\ &\quad \text{where } \delta_p = \min\{\delta_s, \delta_m\}. \end{aligned} \tag{12}$$

Let $(K\zeta\mu_4 R_X + N\mu_2 H_X) = \psi_4(t)$, so that on solving for $N_P(t)$ we get

$$N_p(t) \leq \frac{\Lambda}{\delta_p} + e^{-\delta_p t}\left(N_p(0) - \frac{\Lambda}{\delta_p}\right) \tag{13}$$

Clearly, the malaria parasite populations $S(t)$ and $M(t)$ are bounded above. That is,

$N_P(t) \leq \max\{N_P(0), \Lambda/\delta_p\}$ for all time $t > 0$.

Based on this discussion, we have shown the existence of a bounded positive invariant region for our model system (1). Let us denote this region as $\Omega \in \mathbb{R}_+^7$, where

$$\begin{aligned}\Omega = \Bigg\{ & \left(H, H_X, R, R_X, Z, S, M\right) \in \mathbb{R}_+^7 : N_P(t) \\ & \leq \max\left\{N_P(0), \frac{\Lambda}{\delta_p}\right\}, N_H(t) \\ & \leq \max\left\{N_H(0), \frac{\lambda_h}{\mu_h}\right\}, N_R(t) \\ & \leq \max\left\{N_R(0), \frac{\lambda_r}{\mu_r}\right\}, Z(t) \leq \max\left\{Z(0), \frac{\lambda_z}{\delta_z}\right\}\Bigg\}.\end{aligned} \tag{14}$$

Moreover, any solution of our system (1) which commences in Ω at any time $t \geq 0$ will always remain confined in that region. We therefore deduce that the region Ω is positively invariant and attracting with respect to malaria model (1). Our in-host malaria model (1) is hence well posed mathematically and biologically.

3.1.3. Disease-Free Equilibrium Point. The disease-free equilibrium point, $\mathscr{E}_0$, is the state in which the human host is free of malaria infection. At $\mathscr{E}_0$, the sporozoite recruitment rate, $\Lambda = 0$, and parasite and host-infected compartments have zero values; that is, $S^* = M^* = R_X^* = H_X^* = 0$. Therefore,

$$\begin{aligned}\mathscr{E}_0 &= \left(H^*, H_X^*, R^*, R_X^*, Z^*, S^*, M^*\right) \\ &= \left(\frac{\lambda_h}{\mu_1}, 0, \frac{\lambda_r}{\mu_3}, 0, \frac{\lambda_z}{\delta_z}, 0, 0\right).\end{aligned} \tag{15}$$

3.1.4. In-Host Basic Reproduction Number. The in-host reproduction number of model (1) denoted by R_0 is computed using the technique of the next-generation matrix approach described in [41]. We consider H_X, R_X, S, and M as the parasite infested compartments. Adopting the notations in [41], we generate a nonnegative matrix F of new infections and a nonsingular matrix V, showing the transfer of infections from one compartment to the other as follows:

$$F = \begin{pmatrix} 0 & 0 & \dfrac{\beta_s\lambda_h}{\mu_1} & 0 \\ 0 & 0 & 0 & \dfrac{\beta_r\lambda_r}{\mu_3} \\ 0 & 0 & 0 & 0 \\ 0 & 0 & 0 & 0 \end{pmatrix} \tag{16}$$

and

$$V = \begin{pmatrix} \mu_2 & 0 & 0 & 0 \\ 0 & \mu_4 + \dfrac{\eta\lambda_z}{\delta_z} & 0 & 0 \\ 0 & 0 & \delta_s + \dfrac{\beta_s\lambda_h}{\mu_1} & 0 \\ -N\mu_2 & -K\zeta\mu_4 & 0 & \delta_m + \dfrac{\beta_r\lambda_r}{\mu_3} \end{pmatrix}. \tag{17}$$

The inverse of matrix V is hence given by

$$V^{-1} = \begin{pmatrix} \dfrac{1}{\mu_2} & 0 & 0 & 0 \\ 0 & \dfrac{\delta_z}{\eta\lambda_z + \delta_z\mu_4} & 0 & 0 \\ 0 & 0 & \dfrac{1}{\delta_s + \beta_s\lambda_h/\mu_1} & 0 \\ \dfrac{N\mu_3}{\beta_r\lambda_r + \delta_m\mu_3} & \dfrac{K\zeta\delta_z\mu_3\mu_4}{\left(\beta_r\lambda_r + \delta_m\mu_3\right)\left(\eta\lambda_z + \delta_z\mu_4\right)} & 0 & \dfrac{1}{\delta_m + \beta_r\lambda_r/\mu_3} \end{pmatrix}. \tag{18}$$

The next-generation matrix G, which is the product of matrices F and V^{-1}, works out to be

$$G = \begin{pmatrix} 0 & 0 & \dfrac{\beta_s\lambda_h}{\beta_s\lambda_h + \delta_s\mu_1} & 0 \\ \dfrac{N\beta_r\lambda_r}{\beta_r\lambda_r + \delta_m\mu_3} & \dfrac{K\zeta\beta_r\delta_z\lambda_r\mu_4}{\left(\beta_r\lambda_r + \delta_m\mu_3\right)\left(\eta\lambda_z + \delta_z\mu_4\right)} & 0 & \dfrac{\beta_r\lambda_r}{\beta_r\lambda_r + \delta_m\mu_3} \\ 0 & 0 & 0 & 0 \\ 0 & 0 & 0 & 0 \end{pmatrix}. \tag{19}$$

The in-host basic reproduction number R_0 is the spectral radius of the next-generation matrix G. It can clearly be seen that three of the four eigenvalues of matrix G in (19) have zero values; that is, $\lambda_1 = \lambda_2 = \lambda_3 = 0$. The fourth and largest nonnegative eigenvalue λ_4 becomes the in-host model reproduction number. We therefore have

$$R_0 = \frac{K\beta_r\lambda_r}{(\beta_r\lambda_r + \delta_m\mu_3)} \cdot \frac{\zeta\delta_z\mu_4}{(\eta\lambda_z + \delta_z\mu_4)}. \tag{20}$$

The terms in model R_0 can be interpreted as follows:

(1) The term $K\beta_r\lambda_r/(\beta_r\lambda_r + \delta_m\mu_3)$ represents the expected number of infectious merozoite parasites resulting from bursting blood schizonts at the blood stage of malaria infection.

(2) The second term $\zeta\delta_z\mu_4/(\eta\lambda_z + \delta_z\mu_4)$ represents the expected proportion of merozoites that participate in the cycle of erythrocytic schizogony.

(3) Observe that the terms $(\beta_r\lambda_r)/(\beta_r\lambda_r + \delta_m\mu_3) < 1$ and $(\delta_z\mu_4)/(\eta\lambda_z + \delta_z\mu_4) < 1$. So our $R_0 \leq K\zeta$. This implies that the number of secondary infections during malaria infections is largely influenced by the average number of merozoites released K, from a bursting blood schizont, most of which are responsible for secondary infections at the blood stage.

Despite the inclusion of the liver stage dynamics, it is interesting to observe that the above in-host reproduction number and hence the disease progression are heavily driven by the dynamics at the erythrocytic stage.

In the sections that follow, we shall establish both the local stability and global stability of disease-free equilibrium point (15) of model system (1).

3.1.5. Local Stability of the Disease-Free Equilibrium Point, $\mathscr{E}_0$. The Jacobian matrix of model system (1) evaluated at the disease-free equilibrium $\mathscr{E}_0$ is given by

$$J_1(\mathscr{E}_0) = \begin{pmatrix} -\mu_1 & \frac{\rho_1}{\kappa_1} & 0 & 0 & 0 & -\frac{\beta_s\lambda_h}{\mu_1} & 0 \\ 0 & -\mu_2 & 0 & 0 & 0 & \frac{\beta_s\lambda_h}{\mu_1} & 0 \\ 0 & 0 & -\mu_3 & \frac{\rho_2}{\kappa_2} & 0 & 0 & -\frac{\beta_r\lambda_r}{\mu_3} \\ 0 & 0 & 0 & -\frac{\eta\lambda_z}{\delta_z} - \mu_4 & 0 & 0 & \frac{\beta_r\lambda_r}{\mu_3} \\ 0 & 0 & 0 & \frac{\rho_3}{\kappa_3} & -\delta_z & 0 & 0 \\ 0 & 0 & 0 & 0 & 0 & -\frac{\beta_s\lambda_h}{\mu_1} - \delta_s & 0 \\ 0 & N\mu_2 & 0 & K\zeta\mu_4 & 0 & 0 & -\frac{\beta_r\lambda_r}{\mu_3} - \delta_m \end{pmatrix}. \tag{21}$$

It is clear from the first, third, and fifth columns of matrix (21) that the Jacobian matrix has negative eigenvalues $\lambda_1 = -\mu_1, \lambda_2 = -\mu_3$, and $\lambda_3 = -\delta_z$. Upon deleting the first, third, and fifth rows and columns, matrix (21) is reduced to the following 4×4 matrix:

$$J_2(\mathscr{E}_0) = \begin{pmatrix} -\mu_2 & 0 & \frac{\beta_s\lambda_h}{\mu_1} & 0 \\ 0 & -\frac{\eta\lambda_z}{\delta_z} - \mu_4 & 0 & \frac{\beta_r\lambda_r}{\mu_3} \\ 0 & 0 & -\frac{\beta_s\lambda_h}{\mu_1} - \delta_s & 0 \\ N\mu_2 & K\zeta\mu_4 & 0 & -\frac{\beta_r\lambda_r}{\mu_3} - \delta_m \end{pmatrix}. \tag{22}$$

From row three in (22), $\lambda_4 = -\beta_s\lambda_h/\mu_1 - \delta_s$. We further reduce matrix (22) by deleting row three and column three. So,

$$J_3(\mathscr{E}_0) = \begin{pmatrix} -\mu_2 & 0 & 0 \\ 0 & -\frac{\eta\lambda_z}{\delta_z} - \mu_4 & \frac{\beta_r\lambda_r}{\mu_3} \\ N\mu_2 & K\zeta\mu_4 & -\frac{\beta_r\lambda_r}{\mu_3} - \delta_m \end{pmatrix}. \tag{23}$$

Note from row one of (23) that the fifth eigenvalue $\lambda_5 = -\mu_2 < 0$.

The remaining two eigenvalues can be obtained by reducing matrix (23) into the following 2×2 matrix:

$$J_6(\mathscr{E}_0) = \begin{pmatrix} -\frac{\eta\lambda_z}{\delta_z} - \mu_4 & \frac{\beta_r\lambda_r}{\mu_3} \\ K\zeta\mu_4 & -\frac{\beta_r\lambda_r}{\mu_3} - \delta_m \end{pmatrix}. \tag{24}$$

Using the variable λ, the characteristic polynomial associated with matrix (24) is

$$p(\lambda) = \lambda^2 + A\lambda + B, \tag{25}$$

where

$$A = \delta_m + \frac{\eta\lambda_z}{\delta_z} + \frac{\beta_r\lambda_r}{\mu_3} + \mu_4 \text{ and} \tag{26}$$

$$B = \frac{\eta\delta_m\lambda_z}{\delta_z} + \frac{\eta\beta_r\lambda_r\lambda_z}{\delta_z\mu_3} + \delta_m\mu_4 + \frac{\beta_r\lambda_r\mu_4}{\mu_3} - \frac{K\zeta\beta_r\lambda_r\mu_4}{\mu_3}. \tag{27}$$

The characteristic polynomial (25) has negative roots (eigenvalues) if $A > 0$ and $B > 0$. The coefficient A in (26) is clearly positive. We now need to show that B in (27) is strictly positive if $R_0 < 1$. This is done by expressing the coefficient term B in terms of model R_0 as follows:

$$\begin{aligned} B &= \frac{1}{\delta_z\mu_3}\left[\left(\mu_4\delta_z + \eta\lambda_z\right)\left(\beta_r\lambda_r + \delta_m\mu_3\right) - K\zeta\beta_r\delta_z\lambda_r\mu_4\right], \\ &= \frac{1}{\delta_z\mu_3}\left[\left(\mu_4\delta_z + \eta\lambda_z\right)\left(\beta_r\lambda_r + \delta_m\mu_3\right) \cdot \left[1 - \frac{K\zeta\beta_r\delta_z\lambda_r\mu_4}{\left(\mu_4\delta_z + \eta\lambda_z\right)\left(\beta_r\lambda_r + \delta_m\mu_3\right)}\right]\right], \\ &= \frac{\left(\mu_4\delta_z + \eta\lambda_z\right)\left(\beta_r\lambda_r + \delta_m\mu_3\right)}{\delta_z\mu_3}\left[1 - R_0\right]. \end{aligned} \tag{28}$$

It can clearly be seen from (28) that the coefficient B is positive if and only if $R_0 < 1$. We have thus established the following result.

Theorem 2. *The disease-free equilibrium $\mathscr{E}_0$ is locally asymptotically stable in Ω if $R_0 < 1$. If $R_0 > 1$, then $\mathscr{E}_0$ is unstable.*

Biologically, Theorem 2 implies that malaria infection can be eliminated from the human host when $R_0 < 1$. To ensure that elimination of malaria is independent of the initial sizes of the subpopulations, it is necessary to show that $\mathscr{E}_0$ is globally asymptotically stable in Ω, where the model is mathematically and biologically sensible.

3.1.6. Global Asymptotic Stability of the Disease-Free Equilibrium. Using the results obtained in [42], we show that the malaria-free equilibrium state $\mathscr{E}_0$ is globally asymptotically stable when $R_0 < 1$. We begin by rewriting the model system (1) in pseudotriangular form as follows:

$$\begin{aligned} \dot{X}_1 &= A_1(X)\left(X_1 - X_1^*\right) + A_2(X)X_2, \\ \dot{X}_2 &= A_3(X)X_2, \end{aligned} \tag{29}$$

where X_1 is the vector representing the state of different compartment of liver and blood cells that are not infected and do not transmit malaria infections. X_2 represents the states of malaria parasites and host's cells that are responsible for disease transmission. Hence,

$$\begin{aligned} X &= \left(X_1, X_2\right), \\ X_1 &= \left(H, R, Z\right), \\ X_2 &= \left(H_X, R_X, S, M\right) \text{ and} \\ X_1^* &= \left(\frac{\lambda_h}{\mu_1}, \frac{\lambda_r}{\mu_3}, \frac{\lambda_z}{\delta_z}\right). \end{aligned} \tag{30}$$

From the subsystem X_1, we have

$$A_1(X) = \begin{pmatrix} -\mu_1 & 0 & 0 \\ 0 & -\mu_3 & 0 \\ 0 & 0 & -\delta_z \end{pmatrix} \text{ and}$$

$$A_2(X) = \begin{pmatrix} \frac{\rho_1}{\kappa_1} & 0 & -\frac{\lambda_h}{\mu_1}\beta_s & 0 \\ 0 & \frac{\rho_2}{\kappa_2} & 0 & -\frac{\lambda_r}{\mu_3}\beta_r \\ 0 & \frac{\rho_3}{\kappa_3} & 0 & 0 \end{pmatrix}. \tag{31}$$

A direct computation indicates that the eigenvalue of matrix $A_1(X)$ is real and negative. This shows that the system $\dot{X}_1 = A_1(X)(X_1 - X_1^*) + A_2(X)X_2$ is globally asymptotically stable at the disease-free equilibrium, $\mathscr{E}_0$. Similarly, the subsystem X_2 gives rise to the following matrix $A_3(X)$:

$$A_3(X) = \begin{pmatrix} -\mu_2 & 0 & \beta_s\frac{\lambda_h}{\mu_1} & 0 \\ 0 & -\left(\eta\frac{\lambda_z}{\delta_z} + \mu_4\right) & 0 & \beta_r\frac{\lambda_r}{\mu_3} \\ 0 & 0 & -\left(\beta_s\frac{\lambda_h}{\mu_1} + \delta_s\right) & 0 \\ N\mu_2 & K\zeta\mu_4 & 0 & -\left(\beta_r\frac{\lambda_r}{\mu_3} + \delta_m\right) \end{pmatrix}. \tag{32}$$

It can clearly be seen that $A_3(X)$ is a Metzler matrix: all the off-diagonal elements of $A_3(X)$ are nonnegative. In order to establish the global stability of the disease-free equilibrium, we need to show that the matrix $A_3(X)$

is Metzler stable by providing a proof of the following lemma.

Lemma 3. *Let M be a square Metzler matrix that is block decomposed:*

$$M = \begin{pmatrix} A & B \\ C & D \end{pmatrix}, \tag{33}$$

where A and D are square matrices. The matrix M is Metzler stable if and only if A and $D - CA^{-1}B$ are Metzler stable.

In our case, matrix M is represented by matrix A_3 in (32), so that

$$\begin{aligned} A &= \begin{pmatrix} -\mu_2 & 0 \\ 0 & -\left(\eta\dfrac{\lambda_z}{\delta_z} + \mu_4\right) \end{pmatrix}, \\ B &= \begin{pmatrix} \beta_s\dfrac{\lambda_h}{\mu_1} & 0 \\ 0 & \beta_r\dfrac{\lambda_r}{\mu_3} \end{pmatrix}, \\ C &= \begin{pmatrix} 0 & 0 \\ N\mu_2 & K\zeta\mu_4 \end{pmatrix} \text{ and} \\ D &= \begin{pmatrix} -\left(\beta_s\dfrac{\lambda_h}{\mu_1} + \delta_s\right) & 0 \\ 0 & -\left(\beta_r\dfrac{\lambda_r}{\mu_3} + \delta_m\right) \end{pmatrix}. \end{aligned} \tag{34}$$

Upon computation in Mathematica software, we obtain

$$D - CA^{-1}B = \begin{pmatrix} -\omega_1 & 0 \\ \omega_2 & -\omega_3 \end{pmatrix}, \tag{35}$$

where $\omega_1 = \delta_s + \beta_s(\lambda_h/\mu_1)$, $\omega_2 = N\beta_s\lambda_h/\mu_1$, and $\omega_3 = \delta_m + \beta_r\lambda_r(\eta\lambda_h + (1 - K\zeta)\delta_z\mu_4)/\mu_3(\eta\lambda_z + \delta_z\mu_4)$.

For the matrix $D - CA^{-1}B$ to be Metzler stable, ω_3 should be strictly nonnegative. Therefore, the expression in the numerator

$$\beta_r\lambda_r\left(\eta\lambda_h + (1 - K\zeta)\,\delta_z\mu_4\right) \geq 0. \tag{36}$$

Upon simplification of (36),

$$K\zeta\beta_r\lambda_r\delta_z\mu_4 \leq \beta_r\lambda_r\left(\eta\lambda_h + \delta_z\mu_4\right), \tag{37}$$

$$\left(\frac{\beta_r\lambda_r + \delta_m\mu_3}{\beta_r\lambda_r}\right)\left(\frac{K\zeta\beta_r\lambda_r\delta_z\mu_4}{(\beta_r\lambda_r + \delta_m\mu_3)(\eta\lambda_z + \delta_z\mu_4)}\right) \leq 1, \tag{38}$$

$$\left(\frac{\beta_r\lambda_r + \delta_m\mu_3}{\beta_r\lambda_r}\right)R_0 \leq 1 \tag{39}$$

$$R_0 \leq \frac{\beta_r\lambda_r}{\beta_r\lambda_r + \delta_m\mu_3} < 1. \tag{40}$$

Clearly, matrix A in (34) is Metzler stable. However, the matrix $D - CA^{-1}B$ is Metzler stable if and only if $R_0 < 1$. From Lemma 3, we deduce the following theorem.

Theorem 4. *The malaria-free equilibrium $\mathscr{E}_0$ of model system (1) is globally asymptotically stable if the threshold quantity $R_0 < 1$.*

The above result is quite significant in malaria control. The global stability of the disease-free status would be guaranteed if and only if the in-host basic reproduction number R_0 is less than one. Malaria intervention should therefore focus on eliminating infected erythrocytes and/or malaria merozoites that are responsible for erythropoiesis cycle and invasions at the blood stage.

3.2. The Endemic Equilibrium Analysis. When $R_0 > 1$, the stability of the disease-free equilibrium (15) is violated. A different equilibrium state termed the endemic equilibrium is achieved. Equating to zero the RHS of system (1) and solving for the state variables R, H, Z, S, and M in terms of the infected states H_X and R_X, we obtain the endemic state $\mathscr{E}_1 = (H^*, H_X^*, R^*, R_X^*, Z^*, S^*, \mathrm{M}^*)$, where

$$\begin{aligned} H^* &= \frac{1}{\mu_1}\left\{\lambda_h + \frac{\rho_1 H_X^*}{\kappa_1 + H_X^*} - \mu_2 H_X^*\right\}, \\ S^* &= \frac{\mu_1\mu_2 H_X^*}{\beta_s\left(\lambda_h + \rho_1 H_X^*/\left(\kappa_1 + H_X^*\right) - \mu_2 H_X^*\right)}, \end{aligned} \tag{41}$$

$$\begin{aligned} R^* &= \frac{1}{\mu_3}\left\{\lambda_r + \frac{\rho_2 R_X^*}{\kappa_2 + R_X^*} - \mu_4 R_X^*\right\}, \\ M^* &= \mu_3\left(R_X^*\mu_4 + \frac{\eta R_X^*\left(\rho_3 R_X^*/\left(\kappa_3 + R_X^*\right) + \lambda_z\right)}{\mu_1}\right) \end{aligned} \tag{42}$$

$$Z^* = \frac{1}{\delta_z}\left\{\lambda_z + \frac{\rho_3 R_X^*}{\kappa_3 + R_X^*}\right\} \tag{43}$$

Substituting (41) into the 2^{nd} equation in (1) and simplifying, we obtain the following cubic equation:

$$\alpha_3 H_X^{*3} + \alpha_2 H_X^{*2} + \alpha_1 H_X^* + \alpha_0 = 0, \tag{44}$$

where

$$\begin{aligned} \alpha_3 &= \mu_2^2\beta_s > 0, \\ \alpha_2 &= \mu_2\left(\mu_1\left(-\delta_s\right) - \beta_s\left(\lambda_h - \kappa_1\mu_2 + \Lambda + \rho_1\right)\right), \\ \alpha_1 &= \beta_s\left(\lambda_h\left(\Lambda - \kappa_1\mu_2\right) + \Lambda\left(\rho_1 - \kappa_1\mu_2\right)\right) \\ &\quad - \kappa_1\mu_1\mu_2\delta_s, \text{ and} \\ \alpha_0 &= \kappa_1\Lambda\lambda_h\beta_s > 0. \end{aligned} \tag{45}$$

The number and nature of the roots of (44) are determined by the following discriminant:

$$\begin{aligned} \Delta = {} & 18\alpha_3\alpha_2\alpha_1\alpha_0 - 4{\alpha_2}^3\alpha_0 + {\alpha_2}^2{\alpha_1}^2 - 4\alpha_3{\alpha_1}^3 \\ & - 27{\alpha_3}^2{\alpha_0}^2. \end{aligned} \tag{46}$$

So

(i) if $\Delta = 0$, then (44) has multiple real roots and only one endemic equilibrium would exist,

(ii) if $\Delta < 0$, then (44) has 1 real root and a complex conjugate root and hence only one endemic equilibrium,

(iii) if $\Delta > 0$, then (44) has 3 distinct real roots and so there is more than one endemic equilibrium when $R_0 > 1$ for model system (1).

Analysis under (46) implies that, in the absence of external interventions in the form of antimalarial treatment, there will always be some infected hepatocytes during malaria infection. We then evaluate the possible values of the state variable R_X at equilibrium by substituting expressions in (42) and (43) into the 4^{th} equation in (1). After simplification in Mathematica software, we obtain the following cubic equation:

$$R_X^* \left(\theta_3 R_X^{*3} + \theta_2 R_X^{*2} + \theta_1 R_X^* + \theta_0\right) = 0, \tag{47}$$

where

$$\begin{aligned}
\theta_3 &= -\mu_4\beta_r\left(\mu_1\mu_4 + \eta\left(\rho_3 + \lambda_z\right)\right) < 0,\\
\theta_2 &= \eta\rho_3\left(\beta_r\left(-\kappa_2\mu_4 + \rho_2 + \lambda_r\right) - 1\right) + \left(\mu_1\mu_4 + \eta\lambda_z\right)\\
&\quad \cdot \left(\beta_r\left(-\left(\kappa_2 + \kappa_3\right)\mu_4 + \rho_2 + \lambda_r\right) - 1\right),\\
\theta_1 &= \eta\kappa_2\rho_3\left(\beta_r\lambda_r - 1\right) - \left(\mu_1\mu_4 + \eta\lambda_z\right)\left(\kappa_3\right.\\
&\quad \left. + \kappa_2\left(\beta_r\left(\kappa_3\mu_4 - \lambda_r\right) + 1\right) + \kappa_3\left(-\beta_r\right)\left(\rho_2 + \lambda_r\right)\right),\\
\theta_0 &= \kappa_2\kappa_3\left(\beta_r\lambda_r - 1\right)\left(\mu_1\mu_4 + \eta\lambda_z\right).
\end{aligned} \tag{48}$$

Clearly, $R_X^* = 0$ or

$$\theta_3 R_X^{*3} + \theta_2 R_X^{*2} + \theta_1 R_X^* + \theta_0 = 0. \tag{49}$$

The state $R_X^* = 0$ corresponds to a scenario in which there are no parasite-infected red blood cells. This could signify the liver stage of parasite development so that an endemic state $(H^{**}, H_X^{**}, R^{**}, 0, 0, S^{**}, 0)$ exists. Alternatively, $R_X^* = 0$ could correspond to the disease-free equilibrium point (15) for system (1).

The roots of the cubic equation (49) are given as

$$\begin{aligned}
R_{X1}^* &= -\frac{\kappa_3\left(\mu_1\mu_4 + \eta\lambda_z\right)}{\eta\rho_3 + \mu_1\mu_4 + \eta\lambda_z} < 0,\\
R_{X2,3}^* &= \frac{\left(\beta_r\lambda_r - \kappa_2\mu_4\beta_r + \rho_2\beta_r - 1\right) \pm \sqrt{\Theta}}{2\mu_4\beta_r},
\end{aligned} \tag{50}$$

where

$$\begin{aligned}
\Theta &= 4\mu_4\beta_r\left(\kappa_2\beta_r\lambda_r - \kappa_2\right)\\
&\quad + \left(\beta_r\lambda_r - \kappa_2\mu_4\beta_r + \rho_2\beta_r - 1\right)^2.
\end{aligned} \tag{51}$$

The root $R_{X1}^* < 0$ should be ignored, since all the model state variables are nonnegative for all time $t \geq 0$. This leaves $R_{X2,3}^*$ as the only two possible roots of (49).

From the above discussion, model (1) could experience a single endemic state or multiple endemic states subject to the roots of (44) and (47). If $R_{X2,3}^*$ are real and positive, then one or two endemic equilibrium points are possible for model (1). It is thus evident that the explicit form of the endemic equilibrium state for model (1) is cumbersome. We shall therefore show its existence numerically based on a certain choice of parameter values in Section 4. Note that case (iii) of (46) indicates the possibility of having multiple endemic equilibria and hence the likelihood of experiencing a backward bifurcation phenomenon. This will be investigated in another research paper.

4. Numerical Simulations and Discussions

In this section, we provide some numerical simulations to illustrate the behaviour of model system (1). We carry out model sensitivity analysis and investigate parameter influence on the dynamics of red blood cells, macrophages, and malaria parasites under different conditions on the in-host reproduction number, R_0.

4.1. Sensitivity Analysis. In epidemic modelling, sensitivity analysis is performed to investigate model parameters with significant influence on R_0 and hence on the transmission and the spread of the disease under study [43]. Following [44], the normalised forward-sensitivity index of a variable, $\triangle$, which depends differentially on a parameter, α, is defined as

$$\Upsilon_\alpha^{\triangle} = \frac{\partial\triangle}{\partial\alpha} \times \frac{\alpha}{\triangle}. \tag{52}$$

Using the formulation in (52) and the parameter values in Table 3, the local sensitivity indices (SI) of R_0 (see (20)) relative to the model parameters are calculated in Mathematica software and the results summarised in Table 4. Note that, due to limited data on in-host dynamics, all the parameter values used in evaluating the sensitivity indices are obtained from indicated past literature.

A positive sign on the SI indicates that an increase (decrease) in the value of such a parameter increases (decreases) the value of R_0 and hence the growth of malaria infection. On the other hand, a negative sign is indicative of a parameter that negatively affects R_0. In order to eliminate in-host malaria infection, the in-host reproduction number should be less than one, that is, $R_0 < 1$.

The average number of merozoites released per bursting infected erythrocyte K and the proportion of merozoites that cause secondary invasions at the blood phase ζ are the most sensitive parameters in determining the disease outcomes. They have the highest sensitivity indices of +1.0000. For instance, a 10% increase (decrease) ζ or K generates a 10% increase (decrease) on R_0 and hence malaria infection severity.

The parameters λ_z, η, μ_4, and δ_z occupy the second rank in influencing the model outcomes. An increase in the parameters μ_4 and δ_z is likely to increase the model R_0. On the other hand, an increase in λ_z and η has a direct negative influence on R_0. Macrophages are highly

Table 3: Parameter values used in the numerical simulation and demonstration of the existence of endemic equilibrium point. See Table 2 for detailed parameter descriptions.

Symbol	Interpretation	Value	Source
δ_z	Death rate of macrophages	0.05/day	[19]
δ_s	Death rate of sporozoites	1.2×10^{-11} /day	[20]
η	Elimination rate of IRBCs by macrophages	$10^{-10} cells\mu l^{-1}//day$	[19]
λ_h	Recruitment rate of H	$2.5 \times 10^8 cells/\mu l^{-1}/day$	[21]
ρ_1	Production rate of H due to H_X	$2.5 \times 10^{-5}/day$	[19]
μ_1	Death rate of H	0.029 /day	[20]
Λ	Rate of injection of sporozoites	20 sporozoites/day	[20]
ρ_2	Production rate of RBCs due to IRBCs	$2.5 \times 10^{-5}/day$	[19]
β_s	Hepatocyte invasion rate	$1.0 \times 10^{-6}/sporozoites/day$	[20]
ρ_3	Immunogenicity of IRBCs	$2.5 \times 10^{-5}/day$	[19]
μ_2	Death rate of infected hepatocytes	0.02/day	[20]
κ_1	Inhibition rate	$1\, cells/\mu l^{-1}$	[22]
λ_r	Recruitment rate of RBCs	$2.5 \times 10^8 cells/\mu l^{-1}/day$	[23]
ζ	Merozoites that cause secondary infections	0.726 (unitless)	[24]
μ_3	Death rate of healthy RBCs	0.0083/day	[23]
κ_2	Inhibition rate	$1\, cells/\mu l^{-1}$	[22]
β_r	Invasion rate of RBCs	$2.0 \times 10^{-9}/merozoites/day$	[23]
N	Merozoites per liver schizont	10000/day	[21]
μ_4	Death rate of infected RBCs	0.025/day	[19]
κ_3	Inhibition rate	$1\, cells/\mu l^{-1}$	[22]
δ_m	Death rate of merozoites	48/day	[23]
K	Merozoites per blood schizont	16	[21]
λ_z	Recruitment rate of macrophages	$30/\mu l^{-1}/day$	[19]

Table 4: Sensitivity indices of R_0 relative to the model parameters.

Parameter	SI	Parameter	SI
K	+1.0000	ζ	+1.0000
β_r	+0.920422	μ_3	-0.920422
λ_r	+0.920422	λ_z	-0.998585
μ_4	+0.998585	η	-0.998585
δ_z	+0.998585	δ_m	-0.920422

instrumental in malaria parasite clearance and should be preserved.

The rate of generation of macrophages from the bone marrow, λ_z, together with the rate of phagocytosis of infected red blood cells, η, is likely to decrease, proportionally, the disease progression when they are increased. With increased λ_z, there would be more macrophages to phagocytose and clear the rapidly growing density of blood schizonts. This would negatively affect the erythrocytic schizogony. Decreased clearance rate by macrophages would only guarantee successful multiplication of the merozoites through the erythrocytic schizogonic cycle. The subsequent result is increased concentration of merozoites in the host blood and disease progression to even deadly levels.

The parameters β_r and λ_r increase (or decrease) R_0 when they are increased (or decreased). Epidemiologically, an improved erythrocyte invasion rate, β_r, is likely to generate even more new blood schizonts. This increases parasitemia in the host. A 10% increase (decrease) in β_r would increase (decrease) the threshold parameter R_0 by about +9.2%.

Any therapeutic effort that clears the blood schizonts and the infectious merozoites at the blood stage would definitely guarantee immense reduction in model R_0. Therefore, an increase in the death rate of the infected red blood cells and that of the merozoites is likely to decrease significantly the in-host reproduction number R_0. This can be achieved through the use of effective antimalarials such as the use of artemisinin based combination therapy (ACT) in malaria treatment. Moreover, effective vaccines at the erythrocytic stage could greatly help minimize erythrocyte infection rate β_r.

Since the local sensitivity indices are relatively close, we carry out further investigation on parameter influence on disease progression by generating the partial rank correlation coefficients (PRCCs) for each parameter value in model R_0 in the following section.

4.1.1. Global Sensitivity Analysis. A global sensitivity analysis (GSA) is performed to examine the response of an epidemic model to parameter variation within a wider range of parameter space [45]. Applying the approach in [45], the PRCCs between the in-host basic reproduction number R_0 and each of the parameters in Table 2 are derived. Using 1000 simulations per run of the Latin Hypercube Sampling (LHS) scheme [46], the established PRCCs are derived and presented in Figure 2.

Unlike the results in Table 4, the model parameter with the highest influence on R_0 according to the PRCCs results shown in Figure 2 is the rate of invasion of red blood cells by merozoites, β_r. This is followed closely by the recruitment rate of susceptible red blood cells λ_r from the bone marrow. The second set of parameters that also increase (decrease) model R_0 when they are increased (decreased) are ζ, K, μ_3, and δ_z, respectively.

The merozoites' death rate δ_m, the death rate of IRBCs μ_4, and the rate of elimination of IRBCs by macrophages η are shown to have the highest negative influence on disease progression. Although an increase in μ_4 was shown to decrease disease progression in Table 4, the results from global sensitivity analysis are contradictory. An increase in the death rate of parasitized erythrocytes μ_4 decreases parasitemia and hence disease progression.

Based on these results of sensitivity analysis, we make the following remarks: (1) results of global sensitivity analysis are robust and a lot more realistic for implementation, (2) malaria control should target elimination of merozoites and infected red blood cells, (3) an effective and efficient malaria vaccine that deactivates infectious merozoites could be helpful in limiting erythrocyte invasion rate, and (4) a vaccine that is protective of susceptible erythrocytes could further ensure reduced density of second and future generation of merozoites that are responsible for disease progression.

4.2. Numerical Results. Model system (1) is solved numerically using the package scipy.integrate.odeint in Python language. The simulations are performed to illustrate the possible dynamics of the red blood cells, the malaria parasite, and macrophages. For purposes of these simulations, the initial conditions of the variables are hereby assumed. We note that different dynamics could be achieved for a different set of initial conditions.

For $R_0 < 1$ (see Figure 3), the density of susceptible hepatocyte initially declines as the density of infected hepatocytes rises due to invasion from sporozoites. The host's immune system responds to sporozoite invasion by increasing hepatocyte density that levels off at the disease-free equilibrium point $\mathscr{E}_0$ (see Figure 3(a)). As the sporozoites decline to near zero (see Figure 3(b)), infected hepatocytes decline and stabilize at $\mathscr{E}_0$ in (15).

At the blood stage, the rising density of infected erythrocytes declines in a similar fashion to that of the infective merozoites when $R_0 < 1$ (see Figure 3(c)). The densities of the infected erythrocytes and merozoites approach $\mathscr{E}_0$ asymptotically. On the other hand, we observe that the density of susceptible red blood cells initially diminishes due to infection by merozoites and later rises before it plateaus as shown in Figure 3(c).

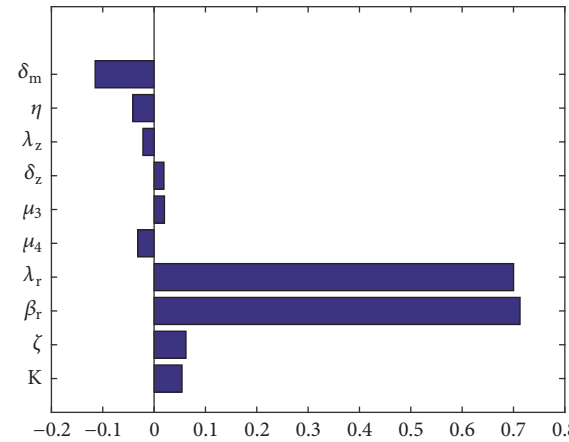

Figure 2: Tornado plots of PRCCs of parameters that influence model R_0 generated using parameter values in Table 3. Parameters with $PRCC > 0$ and $PRCC < 0$ increase and decrease model R_0, respectively.

When $R_0 > 1$, a sharp fall in the density of susceptible hepatocytes in the liver is observed (see Figure 4(a)). This is due to rapid invasion of hepatocytes by the sporozoites. An invasion on susceptible hepatocyte generates a corresponding steady rise in the density of infected hepatocytes (see Figure 4(b)). Owing to natural intervention by the immune system cells, the respective decline and rising levels of susceptible and infected hepatocytes level off and remain relatively constant after the third month. More liver cells are generated to replace infected ones. Figure 4(c) indicates a steady decline in sporozoite density at the liver stage during infections. Invaded hepatocytes burst open to produce merozoites instead of sporozoites and hence the steady decline in sporozoite levels.

Malaria infection dynamics are most rapid in the first 2 weeks within the host liver as illustrated in Figures 4(a), 4(b), and 4(c). This is similar to results in [22, 31]. In the absence of clinical intervention, some of the sporozoites may remain dormant in the human liver and could cause future malaria infections. As the liver schizonts release merozoites into host's blood stream, a rapid decline in the density of red blood cells is observed (see Figure 5(a)). However, the density of infected erythrocytes is noted to rise with equal proportion as shown in Figure 5(b).

An early sharp rise in the density of merozoites in the first one week of the blood stage is noted in Figure 5(c). The density remains high for several weeks and does not decline for the entire infection period of one month. A second-generation merozoite invades other sets of healthy erythrocytes within minutes, leading to an exponential growth in the density of blood schizonts and hence merozoites in the human blood. Without therapeutic intervention, the density of merozoites stabilizes several weeks after infection at the endemic equilibrium point. This is consistent with the findings in [19, 20, 23].

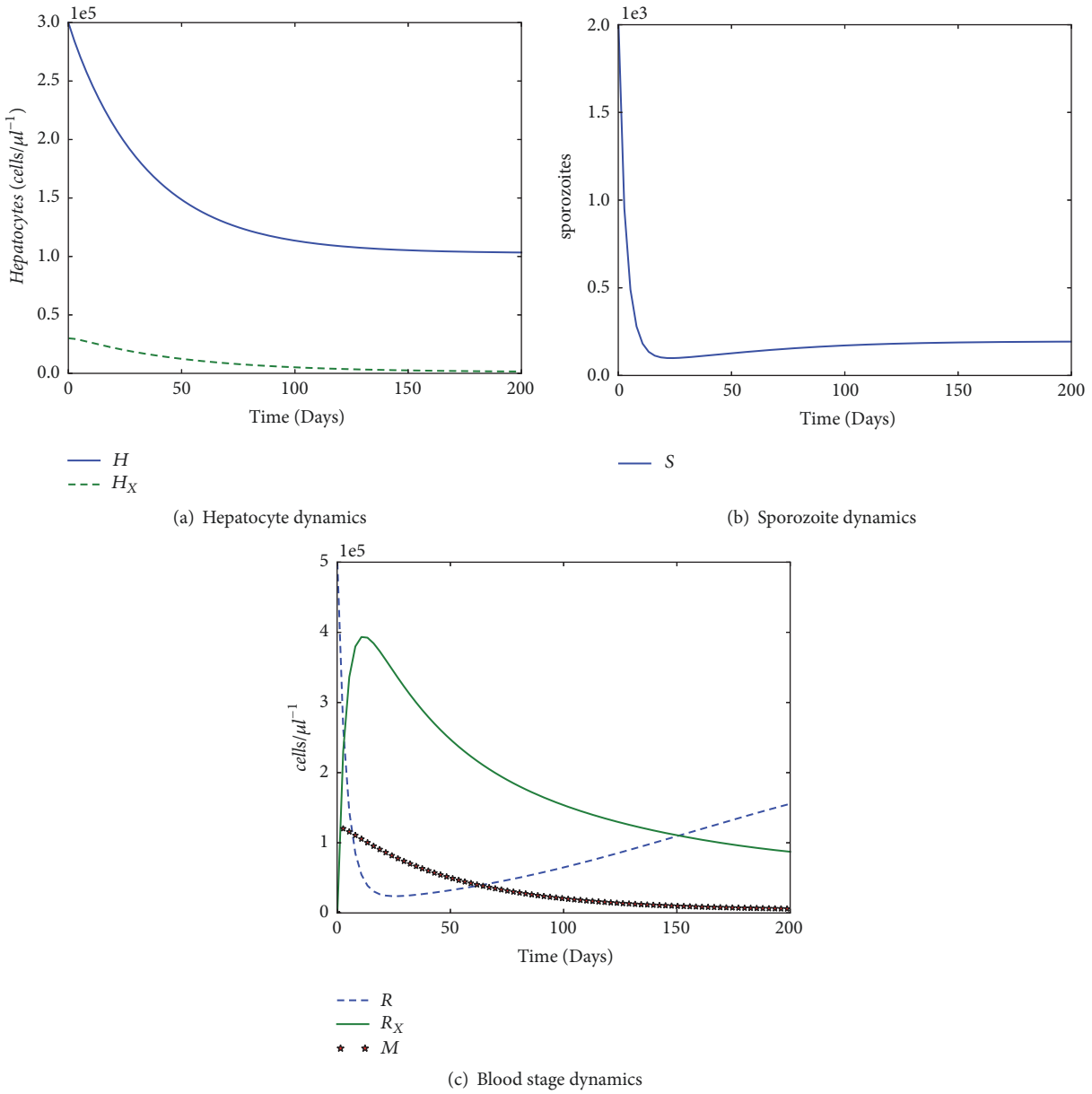

(a) Hepatocyte dynamics

(b) Sporozoite dynamics

(c) Blood stage dynamics

FIGURE 3: Graphs showing the simulation of in-host malaria model (1) when the model $R_0 = 0.22866 < 1$. Figures (a) and (b) show model dynamics at the liver stage. The chosen initial conditions are $H0 = 300000$, $H_X0 = 20000$, $R0 = 500000$, $R_X0 = 50$, $Z0 = 300000$, $S0 = 2000$, and $M = 70$. Used parameter values are given in Table 3.

The invasion of healthy erythrocytes prompts an immune response from host's macrophages. These macrophages phagocyte on the generated blood schizonts. At the onset of erythrocytic infection, several macrophages are generated. The rise in the density of macrophages is proportional to that of infected erythrocytes as shown in Figure 5(d). This rising density is shown to level off after about 16 days at the endemic equilibrium point. It remains high throughout the infection period.

From these discussions, we make the following observations: (1) if $R_0 < 1$, low level malaria infection can easily be contained by the host's defence mechanism and loss of life is less likely; (2) therapeutically, $R_0 < 1$ may be achieved through quick interventions targeting the blood schizonts and the merozoites responsible for secondary infections during the erythrocytic cycle; (3) Figures 4 and 5 prove the existence of malaria endemic equilibrium point.

Hematological parameters such as the density of healthy and infected erythrocytes in malaria hosts have considerable influence on malaria infection and possible impacts [47]. According to WHO [48], hyperparasitemia causes drastic reduction in concentrations of erythrocytes, leading to anaemia among malaria patients. The impacts of increasing the model parameters δ_m and β_r on healthy and infected red blood cells are as shown in Figures 6 and 7, respectively.

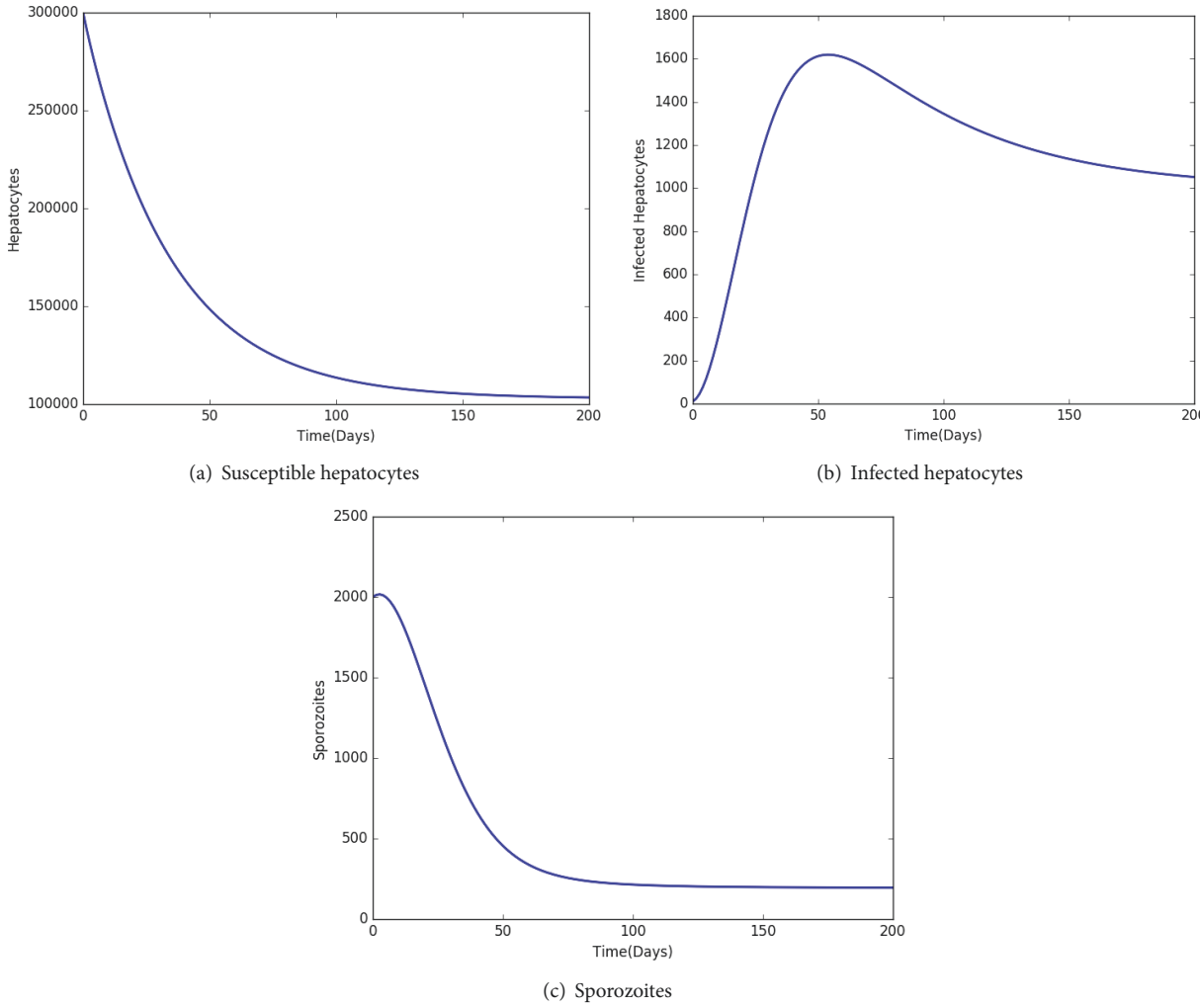

(a) Susceptible hepatocytes

(b) Infected hepatocytes

(c) Sporozoites

FIGURE 4: Graphs showing population dynamics of the liver hepatocytes and malaria sporozoites when $R_0 = 1.58690 > 1$. Used parameter values can be found in Table 3 with the chosen initial conditions described by $H0 = 300000$, $H_X0 = 10$, $R0 = 500000$, $R_X0 = 10$, $Z0 = 10$, $S0 = 2000$, and $M = 20$.

Observe that increased death rate of malaria merozoites δ_m decreases and increases the concentration of parasitized red blood cells and healthy red blood cells, respectively (see Figures 6(a) and 6(b)). Malaria control should thus target the infectious merozoites at the blood stage.

Results in Figure 7(a) indicate that an improved invasion rate by merozoites on susceptible red blood cells causes more loss in healthy erythrocytes. The reverse effect is observed in Figure 7(b), where an increase in the rate of infection of healthy erythrocytes produces a corresponding increase in the density of IRBCs. A keen look at Figure 7(b) reveals that the infected red blood cells begin to appear after about 10–15 days of initial infection. This is consistent with the incubation period of *Plasmodium falciparum* malaria [49].

The severity of malaria infection can easily increase if the density or production of macrophages is compromised [19]. Figure 8(b) shows a near direct relationship on the density of infected red blood cells R_X and the death rate of the macrophages δ_z. An increase in the death of macrophages would propel erythrocytic schizogony and hence increased merozoite numbers in the human blood. A high merozoite density increases the severity of malaria infection. This result is quite vital in malaria intervention, especially with respect to malaria patients who may be suffering from other infections that are deleterious to immune cells. Diseases such as HIV/AIDS greatly weaken the immune system of the patient as crucial immune cells such as macrophages are destroyed. Macrophages are important target cells for HIV-1 virus [50]. During malaria infections, such patients often suffer from severe malaria and should seek immediate medical attention.

Like the senescent red blood cells, aberrant infected erythrocytes formed during malaria infection are eliminated phagocytically by the host's macrophage cells in the red pulp of the spleen [51]. The phagocytic potential of the spleen is vital at the erythrocytic cycle. The higher the phagocytic behaviour of the macrophage, the lower the density of parasitized erythrocytes (see Figure 8(a)). The severity of

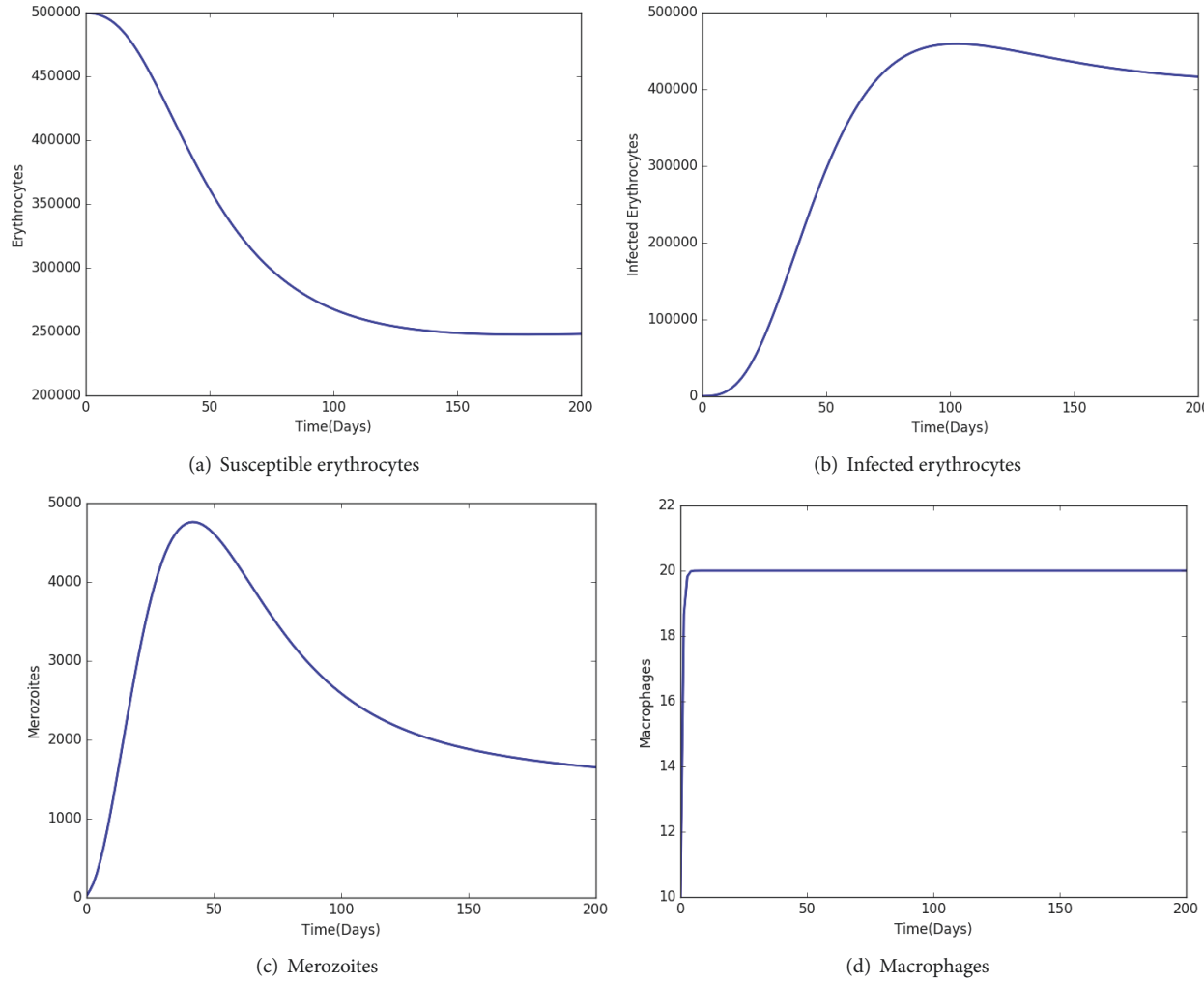

(a) Susceptible erythrocytes

(b) Infected erythrocytes

(c) Merozoites

(d) Macrophages

FIGURE 5: Graphs showing population dynamics of red blood cells, macrophages, and malaria merozoites when $R_0 = 1.58690 > 1$. Simulation parameter values are available in Table 3.

malaria infection increases with decreasing ability of the host's phagocytic merozoites to clear infected red blood cells from circulation during the erythrocytic cycle.

5. Conclusion and Discussion

In this paper, a mathematical model of in-host malaria infection in [21] is extended to include the liver stage of parasite development. Unlike the models in [19, 23, 30], we considered the macrophages as the most effective innate immune cells in eliminating malaria parasites from the human blood circulation. In addition, the liver hepatocytes are assumed to be generated from the bone marrow and through a process of self-regeneration from existing hepatocytes.

We proved that the formulated model is biologically and mathematically well posed in an invariant region Ω. The malaria-free equilibrium is shown to be locally asymptotically stable when the in-host reproduction number is less than unity. The global stability of the malaria-free state is only guaranteed if the threshold quantity R_0 is less than unity.

Our numerical results show that intervention during malaria infection should focus on minimizing merozoite invasion rate on healthy erythrocytes and the density of merozoites in circulation, which are responsible for secondary invasion at the blood stage. In the absence of malaria treatment, the immune cells (macrophages) are shown to be vital in eliminating infected red blood cells at the blood stage. The higher the rate of phagocytosis of infected erythrocytes by macrophages, the lower the density of infected red blood cells and hence malaria parasitemia. Patients suffering from such infections as HIV/AIDS and TB that have deleterious effect on the protective immune cells should seek immediate medical treatment when infected with malaria. Their compromised immune system exposes them to severe malaria attacks and possible untimely death.

For quick and timely reduction of parasitemia, an increased merozoite death rate using antimalarial drugs such as ACT would be necessary. This would further ensure reduced density of infected red blood cells and hence future generation merozoites. By killing a single blood schizont,

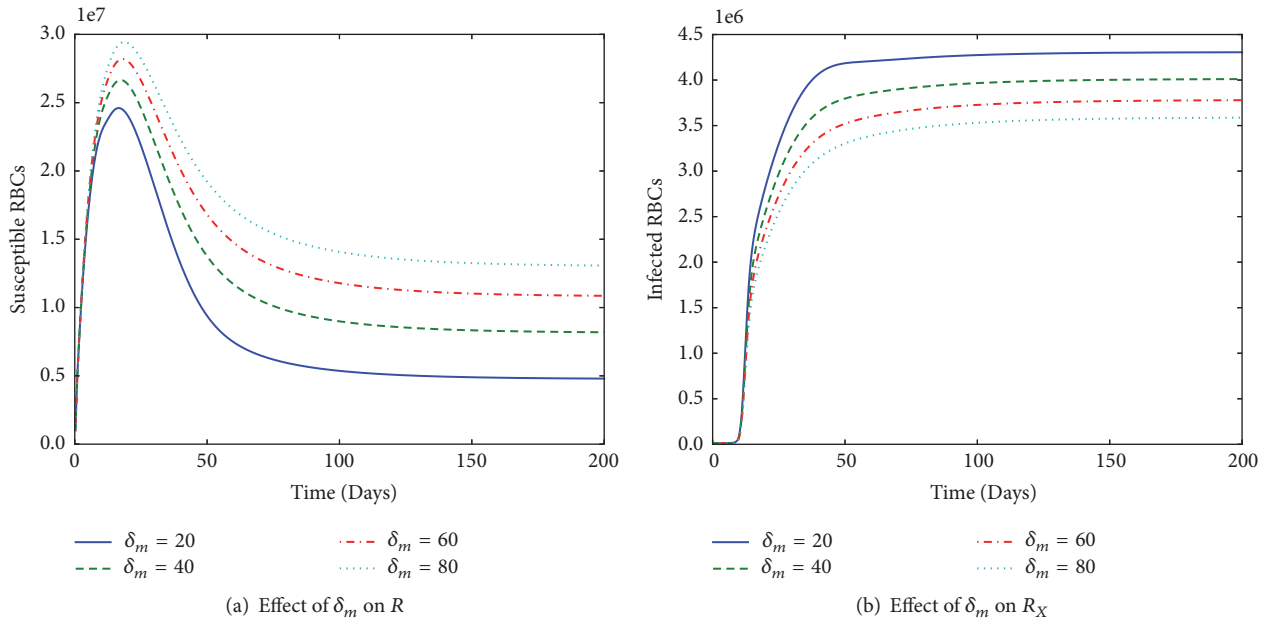

(a) Effect of δ_m on R (b) Effect of δ_m on R_X

FIGURE 6: Graphs showing the behaviour of (a) susceptible RBCs and (b) infected RBCs. They were obtained by varying the death rate of merozoites δ_m from 20 to 80 in steps of 20, while keeping the other parameters (see Table 3) constant.

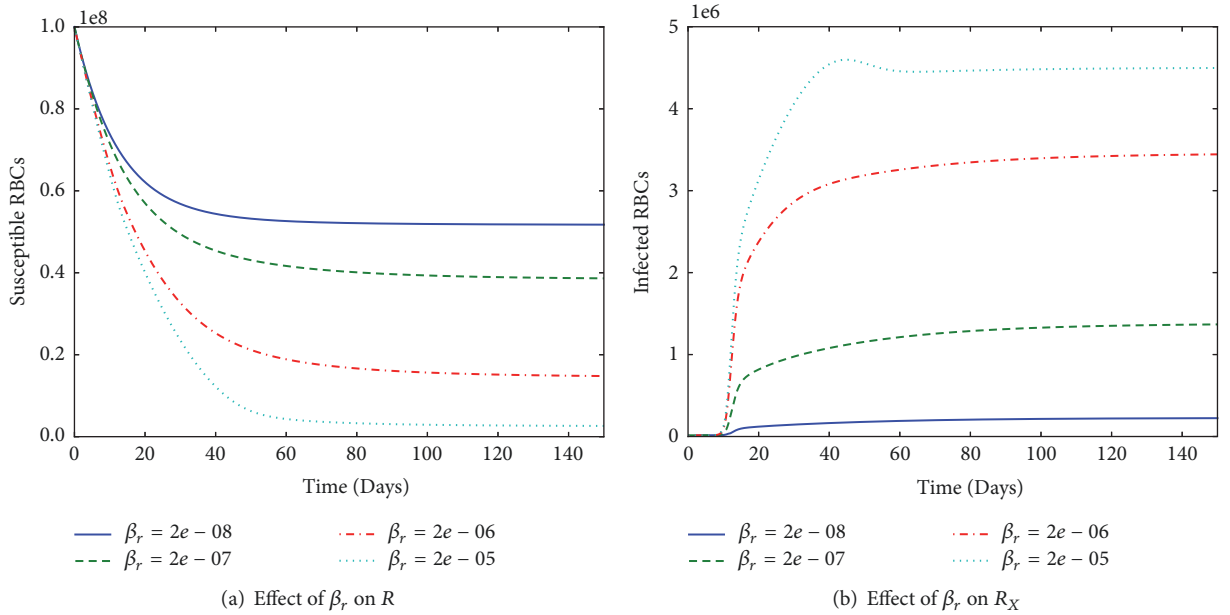

(a) Effect of β_r on R (b) Effect of β_r on R_X

FIGURE 7: Graphs showing the behaviour of (a) susceptible RBCs and (b) infected RBCs. They were obtained by varying the merozoite invasion rate β_r from 2×10^{-8} to 2×10^{-5} in steps of 10^{-1}, while keeping the other parameters in Table 3 constant.

we are likely to avoid the production of sixteen merozoites at maturity. Moreover, an appropriate vaccine that targets erythrocyte invasion process may equally guarantee minimal erythropoiesis. The erythrocyte invasion-avoidance vaccine would minimize the density of infected erythrocytes and hence malaria disease severity. This intervention could help terminate the erythrocytic schizont, leading to minimal parasite transmission to mosquito vector for further development and sexual reproduction.

In this study, drug resistance was not analyzed; this can be considered as a potential area for future investigation.

Conflicts of Interest

The authors declare that there are no conflicts of interest regarding the publication of this article.

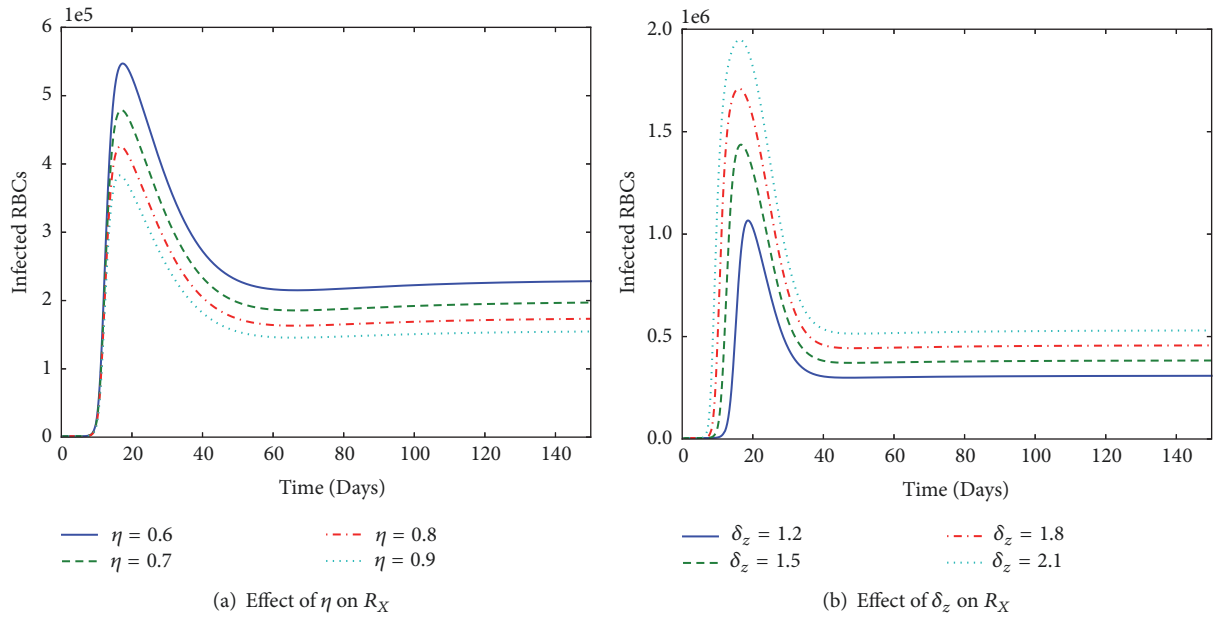

(a) Effect of η on R_X

(b) Effect of δ_z on R_X

FIGURE 8: Graphs showing the effect of varying the rate of phagocytosis of IRBCs by macrophages, η (in (a)), and the effect of increased decay rate of macrophages, δ_z (in (b)), on the behaviour of infected erythrocytes R_X. All parameter values are in Table 3.

Acknowledgments

The authors acknowledge with gratitude the support from the Institute of Mathematical Sciences, Strathmore University, and the National Research Fund (NRF), Kenya, for the production of this manuscript.

References

[1] WHO, *Global Health Observatory (GHO) data: Malaria*, 2017, http://www.who.int/gho/malaria/en/.

[2] WHO, "Fact sheet: World malaria report 2016," http://www.who.int/malaria/media/world-malaria-report-2016/en/.

[3] WHO, "Fact sheet: Malaria," http://www.who.int/mediacentre/factsheets/fs094/en/.

[4] WHO., "Achieving the malaria MDG target: Reversing the incidence of malaria 2000-2015," http://www.who.int/malaria/publications/atoz/9789241509442/en/.

[5] K. Mendis, B. J. Sina, P. Marchesini, and R. Carter, "The neglected burden of *Plasmodium vivax* malaria," *The American Journal of Tropical Medicine and Hygiene*, vol. 64, no. 1-2, supplement, pp. 97–106, 2001.

[6] N. T. Bailey, *The biomathematics of malaria*, Charles Griffin, 1982.

[7] M. M. Mota, G. Pradel, J. P. Vanderberg et al., "Migration of Plasmodium sporozoites through cells before infection," *Science*, vol. 291, no. 5501, pp. 141–144, 2001.

[8] A. M. Vaughan, A. S. I. Aly, and S. H. I. Kappe, "Malaria Parasite Pre-Erythrocytic Stage Infection: Gliding and Hiding," *Cell Host & Microbe*, vol. 4, no. 3, pp. 209–218, 2008.

[9] M. F. Good, H. Xu, M. Wykes, and C. R. Engwerda, "Development and regulation of cell-mediated immune responses to the blood stages of malaria: implications for vaccine research," *Annual Review of Immunology*, vol. 23, pp. 69–99, 2005.

[10] H. H. Diebner, M. Eichner, L. Molineaux, W. E. Collins, G. M. Jeffery, and K. Dietz, "Modelling the transition of asexual blood stages of Plasmodium falciparum to gametocytes," *Journal of Theoretical Biology*, vol. 202, no. 2, pp. 113–127, 2000.

[11] C. Chiyaka, "Using mathematics to understand malaria infection during erythrocytic stages," *NuSpace Institutional Repository*, 2010.

[12] S. H. I. Kappe, K. Kaiser, and K. Matuschewski, "The Plasmodium sporozoite journey: A rite of passage," *Trends in Parasitology*, vol. 19, no. 3, pp. 135–143, 2003.

[13] L. H. Miller, D. I. Baruch, K. Marsh, and O. K. Doumbo, "The pathogenic basis of malaria," *Nature*, vol. 415, no. 6872, pp. 673–679, 2002.

[14] A. D. Augustine, B. F. Hall, W. W. Leitner, A. X. Mo, T. M. Wali, and A. S. Fauci, "NIAID workshop on immunity to malaria: Addressing immunological challenges," *Nature Immunology*, vol. 10, no. 7, pp. 673–678, 2009.

[15] Q. Chen, A. Amaladoss, W. Ye et al., "Human natural killer cells control Plasmodium falciparum infection by eliminating infected red blood cells," *Proceedings of the National Acadamy of Sciences of the United States of America*, vol. 111, no. 4, pp. 1479–1484, 2014.

[16] B. S. Franklin, P. Parroche, M. A. Ataíde et al., "Malaria primes the innate immune response due to interferon-γ induced enhancement of toll-like receptor expression and function," *Proceedings of the National Acadamy of Sciences of the United States of America*, vol. 106, no. 14, pp. 5789–5794, 2009.

[17] D. Z. de Back, E. B. Kostova, M. van Kraaij, T. K. van den Berg, and R. van Bruggen, "Of macrophages and red blood cells; A complex love story," *Frontiers in Physiology*, vol. 5, article 9, 2014.

[18] K. Chotivanich, R. Udomsangpetch, R. McGready et al., "Central role of the spleen in malaria parasite clearance," *The Journal of Infectious Diseases*, vol. 185, no. 10, pp. 1538–1541, 2002.

[19] C. Chiyaka, W. Garira, and S. Dube, "Modelling immune response and drug therapy in human malaria infection," *Computational and Mathematical Methods in Medicine. An Interdisciplinary Journal of Mathematical, Theoretical and Clinical Aspects of Medicine*, vol. 9, no. 2, pp. 143–163, 2008.

[20] M. A. Selemani, L. S. Luboobi, and Y. Nkansah-Gyekye, "On stability of the in-human host and in-mosquito dynamics of malaria parasite," *Asian Journal of Mathematics and Applications*, 2016.

[21] J. Tumwiine, J. Y. Mugisha, and L. S. Luboobi, "On global stability of the intra-host dynamics of malaria and the immune system," *Journal of Mathematical Analysis and Applications*, vol. 341, no. 2, pp. 855–869, 2008.

[22] M. A. Selemani, L. S. Luboobi, and Y. Nkansah-Gyekye, "The in-human host and in-mosquito dynamics of malaria parasites with immune responses," *New Trends in Mathematical Sciences*, vol. 5, no. 3, pp. 182–207, 2017.

[23] Y. Li, S. Ruan, and D. Xiao, "The within-host dynamics of malaria infection with immune response," *Mathematical Biosciences and Engineering*, vol. 8, no. 4, pp. 999–1018, 2011.

[24] A. M. Talman, O. Domarle, F. E. McKenzie, F. Ariey, and V. Robert, "Gametocytogenesis: the puberty of *Plasmodium falciparum*," *Malaria Journal*, vol. 3, article 24, 2004.

[25] R. M. Anderson, R. M. May, and S. Gupta, "Non-linear phenomena in host-parasite interactions," *Parasitology*, vol. 99, pp. S59–S79, 1989.

[26] B. Hellriegel, "Modelling the immune response to malaria with ecological concepts: Short-term behaviour against long-term equilibrium," *Proceedings of the Royal Society B Biological Science*, vol. 250, no. 1329, pp. 249–256, 1992.

[27] J. Swinton, "The dynamics of blood-stage malaria: Modelling strain specific and strain transcending immunity. Models for Infectious Human Diseases," in *Their Structure and Relation to Data*, V. Isham and and G. Medley, Eds., pp. 210–212, Cambridge University Press, Cambridge, UK, 1996.

[28] A. M. Dondorp, S. Yeung, L. White et al., "Artemisinin resistance: current status and scenarios for containment," *Nature Reviews Microbiology*, vol. 8, no. 4, pp. 272–280, 2010.

[29] N. J. White, "Antimalarial drug resistance," *The Journal of Clinical Investigation*, vol. 113, no. 8, pp. 1084–1092, 2004.

[30] J. Tumwiine, S. D. Hove-Musekwa, and F. Nyabadza, "A Mathematical Model for the Transmission and Spread of Drug Sensitive and Resistant Malaria Strains within a Human Population," *ISRN biomathematics*, vol. 2014, Article ID 636973, pp. 1–12, 2014.

[31] Z. Tabo, L. S. Luboobi, and J. Ssebuliba, "Mathematical modelling of the in-host dynamics of malaria and the effects of treatment," *Journal of Mathematics and Computer Science*, vol. 17, no. 1, pp. 1–21, 2017.

[32] C. A. W. Bate, J. Taverne, and J. H. L. Playfair, "Malarial parasites induce TNF production by macrophages," *The Journal of Immunology*, vol. 64, no. 2, pp. 227–231, 1988.

[33] M. M. Elloso, H. C. Van Der Heyde, J. A. Vande Waa, D. D. Manning, and W. P. Weidanz, "Inhibition of Plasmodium falciparum in vitro by human $\gamma\delta$ T cells," *The Journal of Immunology*, vol. 153, no. 3, pp. 1187–1194, 1994.

[34] V. V. Ganusov, C. T. Bergstrom, and R. Antia, "Within-host population dynamics and the evolution of microparasites in a heterogeneous host population," *Evolution*, vol. 56, no. 2, pp. 213–223, 2002.

[35] I. M. Rouzine and F. E. McKenzie, "Link between immune response and parasite synchronization in malaria," *Proceedings of the National Acadamy of Sciences of the United States of America*, vol. 100, no. 6, pp. 3473–3478, 2003.

[36] N. J. White et al., "Malaria pathophysiology," *Malaria, parasite biology, pathogenesis and protection*, pp. 371–385, 1998.

[37] N. Fausto, J. S. Campbell, and K. J. Riehle, "Liver regeneration," *Hepatology*, vol. 43, no. 2, pp. S45–S53, 2006.

[38] N. Fausto, "Liver regeneration and repair: hepatocytes, progenitor cells, and stem cells," *Hepatology*, vol. 39, no. 6, pp. 1477–1487, 2004.

[39] J. Crutcher and S. Hoffman, *Malaria. Medical Microbiology*, University of Texas Medical Branch at Galveston, 4th edition, 1996.

[40] S. N. Wickramasinghe and S. H. Abdalla, "Blood and bone marrow changes in malaria," *Baillieres Best Practice and Research in Clinical Haematology*, vol. 13, no. 2, pp. 277–299, 2000.

[41] P. van den Driessche and J. Watmough, "Reproduction numbers and sub-threshold endemic equilibria for compartmental models of disease transmission," *Mathematical Biosciences*, vol. 180, pp. 29–48, 2002.

[42] J. C. Kamgang and G. Sallet, "Global asymptotic stability for the disease free equilibrium for epidemiological models," *Comptes Rendus Mathématique. Académie des Sciences. Paris*, vol. 341, no. 7, pp. 433–438, 2005.

[43] N. Chitnis, J. M. Hyman, and J. M. Cushing, "Determining important parameters in the spread of malaria through the sensitivity analysis of a mathematical model," *Bulletin of Mathematical Biology*, vol. 70, no. 5, pp. 1272–1296, 2008.

[44] L. Arriola and J. Hyman, "Lecture notes, forward and adjoint sensitivity analysis: with applications in dynamical systems," *Linear Algebra and Optimisation Mathematical and Theoretical Biology Institute*, 2005.

[45] J. Wu, R. Dhingra, M. Gambhir, and J. V. Remais, "Sensitivity analysis of infectious disease models: Methods, advances and their application," *Journal of the Royal Society Interface*, vol. 10, no. 86, article 1018, 2013.

[46] M. Stein, "Large sample properties of simulations using Latin hypercube sampling," *Technometrics. A Journal of Statistics for the Physical, Chemical and Engineering Sciences*, vol. 29, no. 2, pp. 143–151, 1987.

[47] L. M. Erhart, K. Yingyuen, N. Chuanak et al., "Hematologic and clinical indices of malaria in a semi-immune population of Western Thailand," *The American Journal of Tropical Medicine and Hygiene*, vol. 70, no. 1, pp. 8–14, 2004.

[48] WHO, "Severe and complicated malaria," *Transactions of the Royal Society of Tropical Medicine and Hygiene*, vol. 84, pp. 1–65, 1990.

[49] W. E. Collins and G. M. Jeffery, "Plasmodium malariae: Parasite and disease," *Clinical Microbiology Reviews*, vol. 20, no. 4, pp. 579–592, 2007.

[50] T. Shiri, W. Garira, and S. D. Musekwa, "A two-strain HIV-1 mathematical model to assess the effects of chemotherapy on disease parameters," *Mathematical Biosciences and Engineering*, vol. 2, no. 4, pp. 811–832, 2005.

[51] J. Krücken, L. I. Mehnert, M. A. Dkhil et al., "Massive destruction of malaria-parasitized red blood cells despite spleen closure," *Infection and Immunity*, vol. 73, no. 10, pp. 6390–6398, 2005.